Published in final edited form as:
Urology. 2009 December ; 74(6): 1351–1357. doi:10.1016/j.urology.2009.04.090.

Diagnosis of Bladder Cancer with MEMS-based Cystoscopic Optical Coherence Tomography

Hugang Ren[1], **Wayne C. Waltzer**[2], **Rahuldev Bhalla**[2], **Jingxuan Liu**[3], **Zhijia Yuan**[1], **Christopher S.D. Lee**[2], **Frank Darras**[2], **David Schulsinger**[2], **Howard L. Adler**[2], **Jason Kim**[2], **Alek Mishail**[2], and **Yingtian Pan**[1,*]

[1]Department of Biomedical Engineering, SUNY at Stony Brook, Stony Brook, NY 11794

[2]Department of Urology, SUNY at Stony Brook, Stony Brook, NY 11794

[3]Department of Pathology, SUNY at Stony Brook, Stony Brook, NY 11794

Abstract

Purpose—We examined the utility and potential limitations of MEMS (Microelectro-mechanical systems) based spectral-domain cystoscopic optical coherence tomography (COCT) to improve the diagnosis of early bladder cancer.

Materials and Methods—OCT catheter was integrated into the single instrument channel of a 22Fr cystoscope to permit white-light guided COCT over a large field of view of 4.6mm wide and 2.1mm deep per scan at 8 frames/s and 10um resolution. Intraoperative COCT diagnosis was performed in 56 patients, with a total of 110 lesions examined and compared with biopsied histology.

Results—The overall sensitivity of COCT (94%) was significantly higher than cystoscopy (75%, p=0.02) and voided cytology (59%, p=0.005); the major enhancement over cystoscopy was for low-grade pTa-1 cancer and carcinoma in situ (p<0.018). The overall specificity of COCT (81%) was comparable to voided cytology (88.9%, p=0.49), but significantly higher than cystoscopy (62.5%, p=0.02).

Conclusions—MEMS-based COCT, owing to its high resolution and detection sensitivity and large field of view, offers great potential for 'optical biopsy' to enhance the diagnosis of non-papillary bladder tumors and their recurrences and to guide bladder tumor resection.

Keywords

Bladder cancer; Cystoscopic optical coherence tomography; Microelectromechanical systems mirror

INTRODUCTION

Carcinoma or cancer that originates in the urothelium is the 5th most common type of cancer with estimated 68,810 new cases and 14,100 deaths in the US in 2008[1]. Most transitional cell

*Corresponding authors: Yingtian Pan, PhD, Associate Professor, Department of Biomedical Engineering, Stony Brook University, HSC T18, Rm. 030B, Stony Brook, NY 11794-8181, Tel: (631) 444-1451, yingtian.pan@sunysb.edu. Wayne C. Waltzer, MD, Professor and Chair, Department of Urology, Stony Brook University, HSC T09, Rm. 040, Stony Brook, NY 11794-8093, Tel: (631) 444-3642, wwaltzer@notes.cc.sunysb.edu.

carcinomas (TCC) are curable if diagnosed and treated early. However, early diagnosis of TCC, in particular, carcinoma in situ (CIS) remains a clinical challenge[2]. For example, urine cytology, FISH and BTA are unable to provide sufficient sensitivity (~50%) for low-grade TCC[3–5]; Radiologic imaging by way of IVP, CT, MRI fail to detect early-stage bladder cancer due to limited resolution[2]. Cystoscopy is currently the gold standard that has proven highly effective for the diagnosis of papillary TCC; however, as an *en face* imaging modality, it often cannot differentiate non-papillary TCC especially CIS which may have a normal appearance from benign inflammatory lesions and relies on random biopsy, resulting in a low diagnostic sensitivity and specificity (e.g., 30–60%)[5–6]. Therefore, a more effective imaging technique that can see below the bladder surface at a high resolution is highly desirable to enhance the current cystoscopic procedures to diagnose and locate flat malignant lesions (e.g., non-papillary TCC, CIS), guide TURBT, and detect recurrent tumor following transurethral resection.

Optical coherence tomography (OCT) is a new imaging technique that enables cross-sectional imaging of biological tissue at a resolution 10 times higher than clinical ultrasound. In addition to successful clinical adoption in ophthalmology, OCT can be integrated with conventional endoscopy to permit high-resolution *in vivo* imaging of intraluminal tracts (e.g., bladder). Recent preclinical animal and human studies demonstrate the potential of OCT for detecting bladder cancer.[7–11] We developed a microelectromechanicalsystem (MEMS) mirror based spectral-domain OCT cystoscopy (COCT) to improve the image resolution, detection sensitivity, imaging rate and field of view (FOV), all of which are critical to in vivo bladder cancer diagnosis[12]. Here, we present a pilot study based on intraoperative cystoscopy for patients suspected of bladder tumors. The diagnoses of COCT were compared with other clinical data such as white-light cystoscopy, histology and voided cytology, so that the utility and potential limitations of MEMS-based COCT for bladder cancer diagnosis may be examined.

MATERIALS AND METHODS

Patient

COCT was performed in the first 56 consecutive subjects, including 46 (82.1%) male and 10 (17.9%) female patients (median 70 in the 25–75% range), suspected of bladder cancer and scheduled to undergo intraoperative cystoscopy. These patient cohorts comprised 24 (35.5%) for possible bladder biopsy (e.g., due to positive cytology, hematuria, or suspicious outpatient cystoscopy) and 32 (47.1%) for possible TURBT among which 12 (17.6%) patients underwent repeated surveillance cystoscopy due to suspected recurrence post intravesicle therapy with mitomycin or BCG, totaling 68 cases. All of the studies were performed after approval by the Stony Brook University Institutional Review Board and patients' informed consents. Healthy control subjects were not recruited for this study.

COCT

Our techniques for MEMS-based spectral-domain cystoscopic OCT have been reported previously[12]. Fig.1 illustrates the image station and OCT cystoscope used in this study. A broadband near infrared (NIR) laser at wavelength λ=1320nm with a spectral bandwidth of $\Delta\lambda$=90nm was used to illuminate the fiberoptic spectral-domain OCT system (SDOCT) and a green laser (532nm) was coupled for endoscopic visual guidance. Unlike previous time-domain OCT techniques, SDOCT circumvented the need for mechanical axial scan by virtue of spectral interferometry[13], thus significantly increasing imaging rate and dynamic range[12], crucial to *in vivo* COCT diagnosis. The sample arm of the OCT system was connected to an OCT catheter integrated via the instrument channel into a 22Fr cystoscope which focused the incident NIR light onto the bladder lumen and collected backscattering from different depths within bladder

wall to recombine with the reference light to obtain a depth profile (A-scan) using a 1D spectral camera. Steering of light laterally with a MEMS mirror in OCT catheter following each A-scan facilitated 2D and 3D COCT imaging. Recent technological advances in high-performance MEMS mirror and SDOCT led to improved imaging rate (8fps), dynamic range (>110dB) and resolution (~10μm), and a larger FOV ($2.1\times4.8mm^2$ in the vertical and lateral directions). The dual-imaging capability permitting white-light or fluorescence guided COCT greatly improves the diagnostic efficacy[10].

Clinical Examination

With the patient under general anesthesia, COCT diagnosis was performed prior to possible biopsy or TURBT treatment. Suspicious lesions, including base and transitional area to the adjacent normal mucosa were examined first, followed by sequential COCT scans of nonspecific or normal-appearing areas (i.e., bladder mapping). COCT diagnosis was given instantaneously using the following criteria: 1) a lesion with diminishing underlying morphology and increased urothelial heterogeneity (e.g., over 3-fold thickened urothelium with varied local backscattering such as fibrovascular cores) was considered to be positive, 2) an area with clearly delineated and uniform urothelium (including inflammatory lesions in the underlying layers) was considered to be negative, and 3) a lesion with ultrahigh surface reflection and missing underlying morphology (e.g., necrosis or scar from prior TURBT) was considered to be negative. The duration of COCT diagnosis was less than 10 minutes per case. Routine cystoscopic evaluation was performed (by urologists only) regardless of COCT diagnosis (by urologists/OCT researchers). Subsequent pathological findings in these lesions, from either random biopsy or TURBT were identified while blind to prior clinical data (e.g., COCT, cystoscopy, cytology), and staged and graded by an independent pathologist. The histological image was then compared with the corresponding COCT cross-section whose surface image (cystoscopy) was cropped from the synchronized video clip.

Statistical Analysis

The sensitivities and specificities of voided cytology, cystoscopy and COCT for detection of bladder cancer were computed with the final biopsed histological diagnosis serving as the gold standard. Their values were compared using chi-squares test or Fisher's exact test, with $p<0.05$ considered statistically significant.

RESULTS

For all 68 intraoperative cases, no complications were observed. Among 36 cancer cases confirmed by histology, 34 were detected by COCT, 27 by cystoscopy, and only 17 were identified by cytology; whereas for all 32 histologically confirmed benign cases, 26 were detected by COCT, 20 by cystoscopy, and 24 identified by cytology. The detailed cancer diagnostic statuses calculated on per patient/case bases are indicated in Tab.1(a). The positive and negative predictive values (PPV, NPV) were calculated accordingly as 85% and 93% for COCT, 64% and 65% for cystoscopy, and 85% and 63% for cytology.

COCT identification of normal bladder was based on high-resolution delineation of bladder morphology. As shown in Fig.2(b), urothelium (U) appears as a thin, uniform and low-scattering superficial layer, lamina propria (LP) – composed of mostly collageneous fibers – as highly scattering and heterogeneous, and upper muscularis (M) as largely bifurcated collagen bundles, correlating well with histology (c). The urothelial thickness measured by COCT (89 ± 8.3μm) closely matched that of histology (82.1 ± 9.7μm) and the inter-patient variation was found insignificant ($p>0.82, n=25$) if the bladder was distended properly, thus providing an important landmark for OCT diagnosis. For instance, the majority of inflammatory lesions might exhibit decreased LP scattering as a result of cystitis, edema or

vasodilatation, but their urothelium remained thin, uniform and could thus be identified. Among the 6 false-positive lesions by COCT, 5 were lesions with reactive giant cell components and scar tissue or metaplasia, and 1 was necrosis mixed with fat tissue, all of which exhibited architectural similarity to TCC.

COCT identification of TCC was based on enhanced urothelial heterogeneity and/or urothelial thickening attributed to random excessive growth of urothelial neoplasm. Fig.2(E) shows the result of a typical papillary TCC (pT1LG). Compared to normal bladder in Fig.2(B), the architectural boundaries between U, LP and M were disrupted in the bladder tumor. The large FOV of MEMS COCT permitted clear identification between TCC and the surrounding normal bladder, thus potentially allowing precise guidance for TURBT. In contrast to previous preclinical study[12], 76% of human TCC exhibited no significant increase in backscattering but rather enhanced urothelial heterogeneity as indicated by the arrows. It is noteworthy that the stratified architectures (LP, M) underneath the TCC diminished, thus potentially compromising the staging ability of COCT for large papillary TCC to pT1 or lower stage. For instance, COCT could stage this TCC as greater than T1 but was uncertain to differentiate it as T1 or T2. Among all 25 papillary TCC cases, COCT detected 24 (96%) but missed 1 close to bladder neck; while cystoscopy detected all 25 (100%).

Detection of recurrent tumor remains an unsolved clinical challenge for surveillance cystoscopy because bladder architecture was drastically altered by previous TURBT. Fig.3(B) demonstrated the great potential of COCT to differentiate recurrent TCC from scar or necrosis because the latter exhibited excessive surface reflection with no underlying morphology. Among 4 of the 12 surveillance cases with recurrent cancers, COCT detected all 4 cases while cystoscopy missed 2. On the other hand, 5 of 6 false positive diagnoses of COCT were associated with previous resections, and 9 of 15 cases were for cystoscopy. In addition, Fig.3 (E) exemplifies the result of a CIS which remains a critical problem for clinical diagnosis due to its non-specific appearance under cystoscopy Fig.3(D). The lesion under COCT showed no obvious urothelial thickening; instead, the backscattering decreased slightly in the urothelium (U*) but diminished drastically in the underlying LP likely due to coexisting inflammatory response so that the boundary between U'-LP was hardly distinguishable, which was later confirmed by histology Fig.3(F). COCT detected 8 out of 9 histologically confirmed CIS lesions; in comparison, cystoscopy only detected 2.

A total of 110 lesions were biopsied for histological analysis following COCT and cystoscopy diagnoses and entered as gold standard for statistical calculation. The diagnostic status calculated on a per lesion basis was summarized in Tab.1(b), which demonstrated the utility of MEMS COCT to significantly enhance the sensitivity ($p<0.018$) of cystoscopy for superficial, low-grade tumors (pTa-1LG) and CIS (Tis), and of cytology for pTa-1LG tumors ($p<0.001$).

DISCUSSION AND CONCLUSIONS

Early diagnosis transitional cell carcinoma remains a clinical challenge[2]. Cytology is highly sensitive in high-grade bladder tumor (e.g., HG or CIS)[3], yet it relies on other imaging techniques to locate the cancerous lesions. White-light cystoscopy is currently gold standard for bladder cancer diagnosis and has proven highly effective for large papillary tumors as exemplified in Tab.1. However, cystoscopy as an *en face* imaging modality can miss small sessile low-grade TCC and CIS which may appear normal or nonspecific, and relies on random biopsy for a conclusive diagnosis[2]. On the other hand, disrupted (altered) bladder surface by previous TURBT may result in difficulty differentiating recurrent tumors from scar, necrotic tissue or other inflammatory reactions. Interestingly, both the merits and limitations of cystoscopy and cytology were well reflected in this study (Tab.1).

In contrast to *en face* imaging, COCT enables cross-sectional imaging over 2mm of depths to delineate bladder epithelium, lamina proper and upper muscularis at a resolution (~10μm) close to histopathology[7], offering great potential to overcome the limitations of conventional cystoscopy and provide more specific diagnosis of early bladder cancer. Previous preclinical and clinical studies demonstrated the feasibility of OCT for bladder cancer diagnosis[8–9]. Here, we present a pilot study to further examine the utility and potential limitations for future clinical diagnosis, in particular, with the advantages resulting from technological advances in SDOCT and MEMS laser scanning catheter for enhanced image sensitivity, speed and increased FOV[12]. The large FOV and of MEMS COCT enabled imaging of the transitional area of the lesion with adjacent normal bladder, critical to enhancing the diagnosis of bladder tumor and imaging guidance of TURBT. The technical modification for our COCT merely involved coupling the OCT catheter via the instrument channel of a conventional 22Fr rigid cystoscope[14]. Moreover, simultaneous surface image guidance and the touch-on-focus capability drastically enhanced the diagnostic efficacy to allow COCT exam of the entire bladder including bladder mapping in less than 10 minutes. For the 68 consecutive cases performed intraoperatively, no adverse events were observed. The COCT system was custom made in our lab for under $20k, which should be affordable for future clinical adoption.

The preliminary clinical results presented in Tab.1 implied that conventional cystoscopy was sufficient for the diagnosis of large papillary tumors (e.g., pT2, pTa-1HG) counting for the majority (21/36(60%) of the cancer cases. The major improvement of COCT was for the diagnosis of superficial pTa-1LG tumors (12/12 vs. 8/12, $p<0.01$) and CIS (8/9 vs. 2/9 lesion based, $p=0.015$). However, it is noteworthy that only 3 pure CIS cases were encountered ($p=0.4$), so more CIS enrollment is needed to evaluate the statistical significance between COCT and cystoscopy on a per case basis (all other 6 CIS cases coexisted with TCC). COCT diagnosis was based on identification of decreased urothelial backscattering with enhanced heterogeneity and diminished U-LP interface[9,12] (Fig.3E), possibly as a result of enlarged nuclei of CIS cells that favor forward scattering. More quantitative study is needed to compare the difference between CIS and flat dysplasia. An ultimate solution will likely demand subcellular imaging differentiation for which our recent invention based on time-lapse ultrahigh-resolution OCT has shown great promise[15].

The rigid COCT missed 1 tumor in retro area close to bladder neck, but this problem can now be tackles by our new flexible COCT catheter. It was interesting to observe the ability of COCT to detect all 6 recurrent TCCs from scar or necrotic lesions induced by previous resections which cystoscopy missed (e.g., 2 pT2 tumors), thereby eliminating unnecessary multiple biopsies and reducing false negative rates of recurrent tumors. Nevertheless, due to disruption of stratified bladder architectures (U, LP, M), 5 out of all 6 false-positive rates of COCT were for surveillance cases. In addition, it is crucial to point out that due to increased urothelial heterogeneity, visualization of the underlying structures (e.g., LP, M) was hampered resulting in limited local staging for large papillary TCC (e.g., pT1 or higher). However, our recent preclinical study[16] suggested that OCT combining with high-frequency ultrasound (HFUS) could compliment each other and thus enhance both bladder cancer diagnosis and extend tumor staging to pT2 or higher.

In conclusion, results of intraoperative MEMS-based COCT on the first 56 patients revealed a significant improvement on the sensitivity (94% vs. 75%) and specificity (81% vs. 53%) over cystoscopy in the diagnosis of bladder cancer ($p<0.05$). The major impact was on small superficial low-grade tumors and carcinoma in situ as well as the detection of recurrent tumors found in surveillance cystoscopy, rendering it a promising adjuvant ‘optical biopsy’ for early detection of non-papillary bladder cancers and image guided therapies. However, considering that intraoperative patients were biased by either more advanced tumors or more complicated cases, the result must be further examined in a more randomized study such as in office

diagnosis which is being evaluated by incorporating our newly developed high-performance flexible COCT technology.

Acknowledgments

This work was supported by NIH 2R01-DK059265 (YP) and Stony Brook University Fusion award (YP). Please address correspondences regarding COCT technology and diagnosis to Y. Pan and other clinical relevance to W. Waltzer.

References

1. http://seer.cancer.gov/csr/1975_2005/results_single/sect_01_table.01.pdf
2. Messing, EM.; Catalona, W. Urothelial tumors of the urinary tract. In: Walsh, PC.; Retik, A.; Vaughan, ED.; Wein, AJ., editors. Campbell's Urology. Vol. 7th ed.. W. B. Saunders Company; 1998. p. 2327-2410.
3. Cajulis RS, Haines GK, Friashidvegi D, et al. Cytology, Flow-cytometry, Image-analysis, and Interphase Cytogenetics by Fluorescence in-situ Hybridization in the Diagnosis of Transitional-cell Carcinoma in Bladder Washes - A Comparative-study. Diagnostic Cytopathology 1995;13:214. [PubMed: 8575280]
4. Sarosdy MF, Schellhammer P, Bokinsky G, et al. Clinical evaluation of a multi-target fluorescent in situ hybridization assay for detection of bladder cancer. J. Urology 2002;168:1950.
5. Leyh H, Marberger M, Conort P, et al. Comparison of the BTA stat (TM) test with voided urine cytology and bladder wash cytology in the diagnosis and monitoring of bladder cancer. European Urology 1999;35:52. [PubMed: 9933795]
6. Kriegmair M, Baumgartner R, Knuchel R, et al. Detection of early bladder cancer by 5-aminolevulinic acid induced porphyrin fluorescence. J. Urology 1996;155:105.
7. Tearney GJ, Brezinski ME, Southern JF, et al. Optical biopsy in human urologic tissue using optical coherence tomography. J Urol 1997;157:1915. [PubMed: 9112562]
8. Pan Y, Lavelle JP, Meyers S, Pirtskhalaishvili G, Zeidel ML, Farkas DL. Detection of tumorigenesis in rat bladders with optical coherence tomography. Med. Phys 2001;28:2432–2440. [PubMed: 11797946]
9. Zagaynova EV, Streltsova O, Gladkova ND, Snopova LB, Gelikonov GV, Feldchtein FI, Morozov AN. In Vivo Optical Coherence Tomography Feasibility for Bladder Disease. J Urology 2002;167:1492–1496.
10. Wang ZG, Durand D, Schoenberg M, Pan YT. Fluorescence Guided Optical Coherence Tomography for the Diagnosis of Early Bladder Cancer in a Rat Model. J. Urology 2005;174:2376–2381.
11. Lerner SP, Goh AC, Tresser NJ, Shen SS. Optical coherence tomography as an adjunct to white light cystoscopy for intravesical real-time imaging and staging of bladder cancer. Urology 2009;72:133–137. [PubMed: 18598789]
12. Wang ZG, Lee CSD, Waltzer WC, Liu JX, Pan YT, et al. In vivo Bladder Imaging with MEMS-based Endoscopic Spectral Domain Optical Coherence Tomography. JBO 2007;12(3):1–9.033703
13. Wojtkowski M, Kowalczyk A, Leitgeb R, Fercher AF. Full range complex spectral optical coherence tomography technique in eye imaging. Opt. Lett 2002;27:1415–1417. [PubMed: 18026464]
14. Pan YT, Xie HK, Fedder GK. Endoscopic optical coherence tomography based on a MEMS mirror. Opt. Lett 2001;26:1966–1968. [PubMed: 18059747]
15. Pan YT, Wu ZL, Yuan ZJ, Wang ZG, Du CW. Subcellular Imaging of Epithelium with Time-lapse Optical Coherence Tomography. JBO Letters 2007;12(5):1–3.050504
16. Yuan ZJ, Wang ZG, Pan YT. High-resolution imaging diagnosis and staging of bladder cancer: A comparison between optical coherence tomography and high-frequency ultrasound. JBO 2008;13(5): 1–10.054007

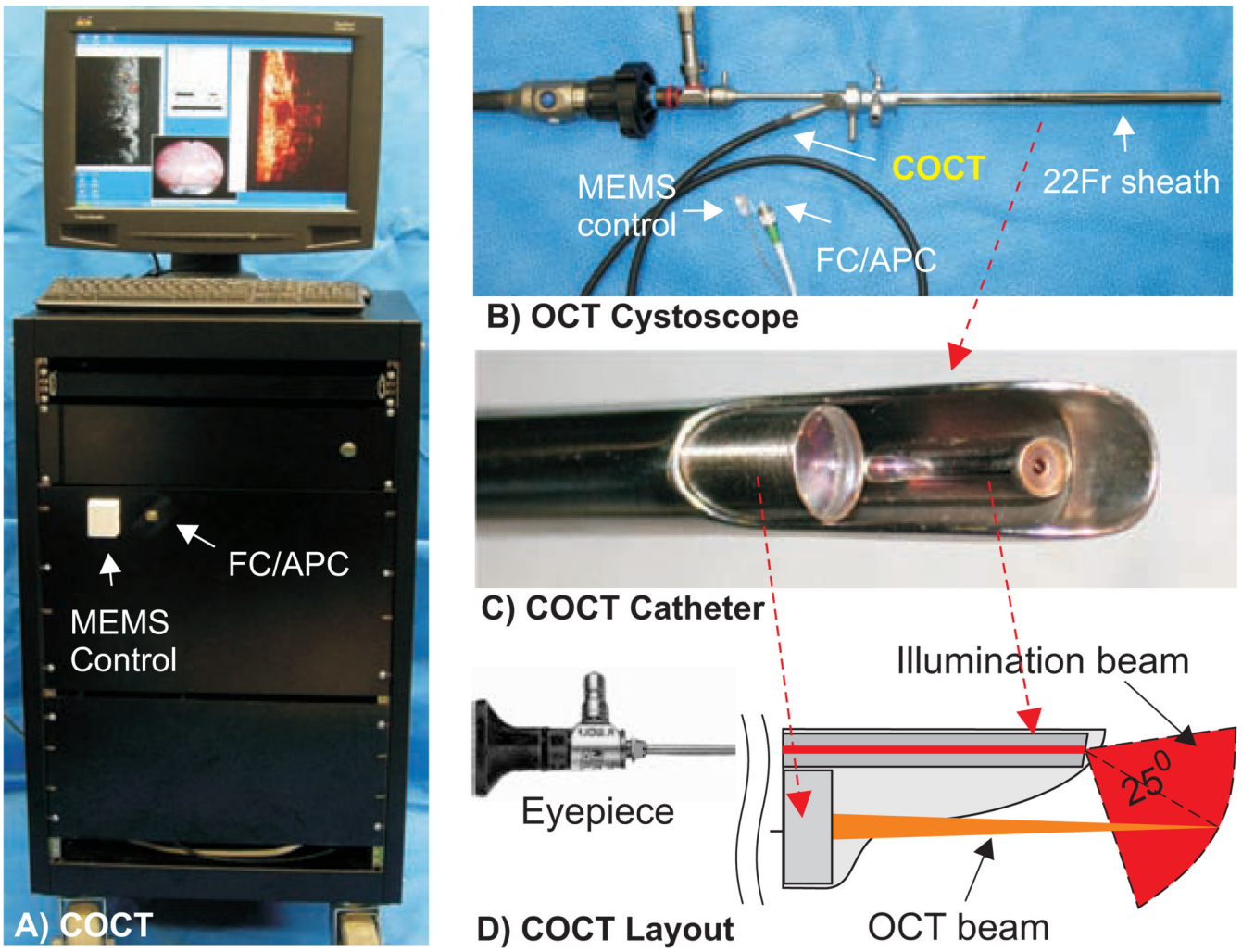

Fig.1.

MEMS-based COCT for *in vivo* bladder cancer diagnosis. A) SDOCT station; B) OCT cystoscope; C, D) COCT catheter that allows white-light or fluorescence image guidance. FC/APC: angle polished fiber connector. Transverse laser scanning (up to 4.8mm) within COCT catheter was facilitated by a CMOS MEMS mirror ($1.1\times1.3mm^2$).

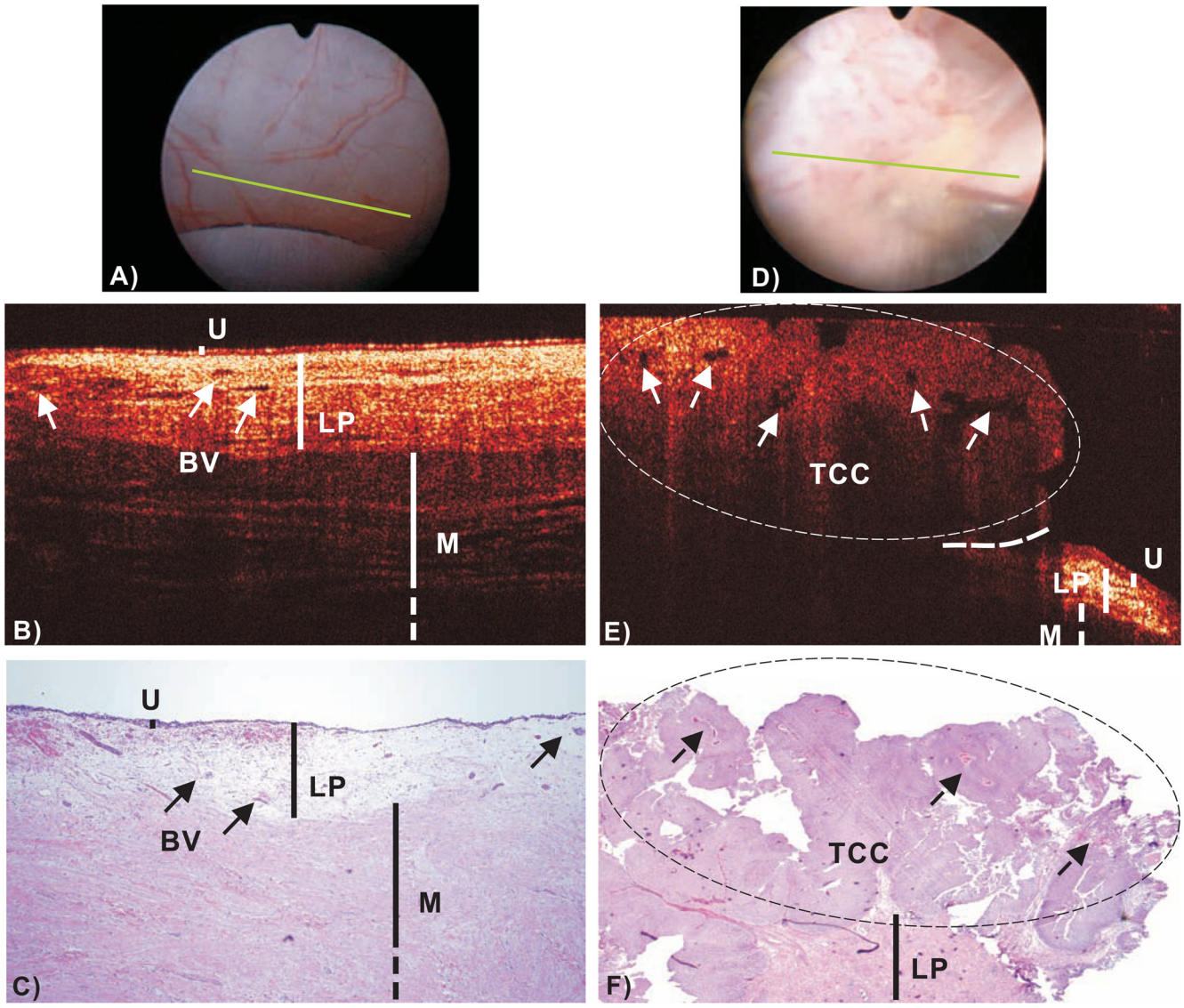

Fig.2.

In vivo surface, cross-sectional COCT and H&E stained histological images of normal human bladder versus a papillary TCC (pT1LG). Image sizes: ~ϕ20mm (A/D) and 4.6mm laterally by 2.1mm axially (B/E, C/F). The morphological details of normal bladder (B), e.g., urothelium (U), lamina propria (LP) and upper muscularis (M) were clearly delineated by OCT based on their backscattering differences; whereas those (e.g., LP, M) underneath papillary TCC (E) diminished. Solid arrows: subsurface blood vessels; dashed arrows: papillary features; dashed circle: TCC (low backscattering), identified by COCT based on increased urothelial heterogeneity; dashed line: boundary with adjacent normal bladder. Diagnoses of the normal bladder: COCT, cystoscopy and histology were all benign, voided cytology was positive. Diagnoses of papillary lesion: COCT, cystoscopy and histology were positive, cytology was benign.

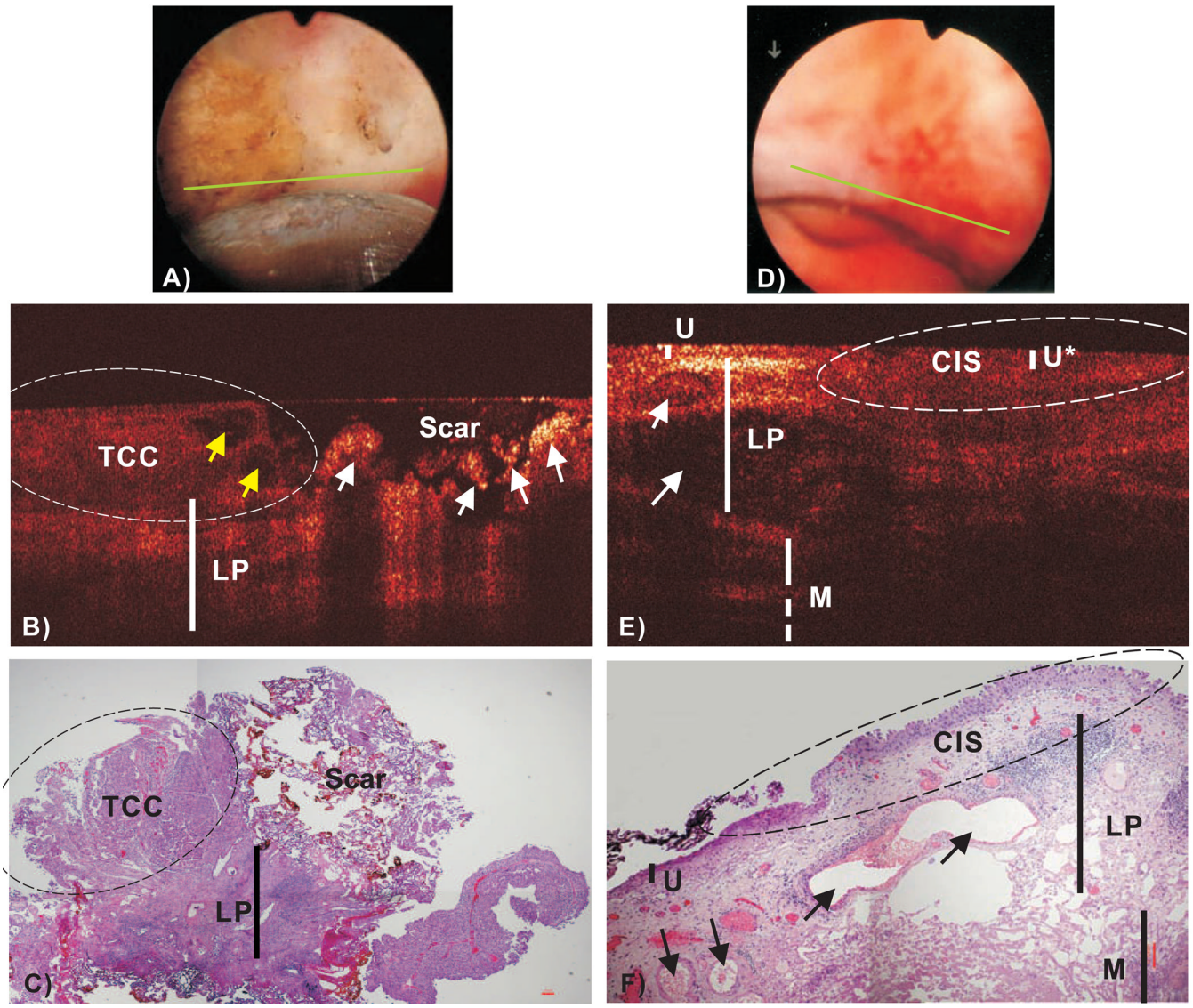

Fig.3.

In vivo surface, COCT and H&E stained histological images of a recurrent TCC post TURBT (A–C) and a CIS (D–F). Yellow and white arrows (B): papillary features and scar or necrotic lesions. COCT differentiation of TCC (left circle) vs. scar (right circle) was based on low-scattering and papillary features in TCC vs. ultrahigh superficial scattering with abruptly diminished underlying architecture in scar or necrotic lesion, which was nonspecific under surface image (a). Arrows (E, F): blood vessels; The morphology (e.g., LP, M) under CIS (U*) diminished. CIS (dashed circle), which was slightly reddish and nonspecific under surface image (D), was low backscattering and identified by COCT based on increased urothelial heterogeneity and less distinguishable U'-LP interface. Diagnoses of TCC/scar: COCT and histology were positive; cystocopy and voided cytology were benign. Diagnoses of CIS: COCT and histology were positive; cystoscopy and voided cytology were benign.

Table 1

Diagnostic sensitivities and specificities:

a) calculated on a per case basis								
Methods		**OCT**	**Cyst**	**Cyto**	**p-values**		
Tumors		**n/N %**	**n/N %**	**n/N %**	**OCT : Cyst**	**OCT : Cyto**	**Cyst : Cyto**
CIS (pTis)		2/3 66.7	0/3 0	3/3 100	0.400	1.000	0.100
pTa-pT1	**LG**	12/12 100	8/12 66.7	0/10 0	0.093	0.0001	0.002
	HG	6/6 100	6/6 100	1/3 33.3	1.000	0.083	0.226
Superficial (<pT2)		20/21 95	14/21 66.7	4/16 25	0.044	0.0001	0.012
≥pT2		14/15 93.3	13/15 86.6	11/13 84.6	1.000	0.583	1.000
Sensitivity		34/36 94.4	27/36 75	17/29 58.6	0.022	0.005	0.160
Specificity		26/32 81.3	17/32 53.2	24/27 88.9	0.017	0.488	0.003
b) calculated on a per lesion basis							
Methods		**OCT**	**Cyst**	**Cyto**	p-values		
Tumors		**n/N %**	**n/N %**	**n/N %**	**OCT : Cyst**	**OCT : Cyto**	**Cyst : Cyto**
CIS (pTis)		8/9 88.9	2/9 22.2	8/8 100	0.015	1.000	0.002
pTa-pT1	**LG**	17/17 100	11/17 64.7	0/14 0	0.018	0.0001	0.0001
	HG	9/9 100	8/9 88.9	4/6 66.7	1.000	0.143	0.525
Superficial (<pT2)		34/35 97	21/35 60	12/28 42.9	0.002	0.0001	0.040
≥pT2		17/18 94.4	16/18 88.9	14/16 87.5	1.000	0.591	1.000
Sensitivity		51/53 96.2	37/53 69.8	26/44 59.1	0.0003	0.0001	0.271
Specificity		51/57 89.5	42/57 73.7	45/48 93.8	0.030	0.436	0.007

* Cyst: cystoscopy, Cyto: cytology; N: total number, LG: low grade, Superficial: all pTis and pTa-pT1 tumors. Cytology data for 12 cases were unavailable.